https://doi.org/10.5194/hess-2024-174
Preprint. Discussion started: 26 July 2024

Hydrology and Earth System Sciences
Discussions

The Value of Hydroclimatic Teleconnections for Snow-based Seasonal Streamflow Forecasting

Atabek Umirbekov[1,4], Mayra Daniela Peña-Guerrero[1,4], Iulii Didovets[2], Heiko Apel[3], Abror Gafurov[3] and Daniel Müller[1, 4, 5]

[1] Leibniz Institute of Agricultural Development in Transition Economies (IAMO), Theodor-Lieser-Str. 2, 06120 Halle (Saale), Germany
[2] Potsdam Institute for Climate Impact Research (PIK), Telegrafenberg A 31, 14473 Potsdam, Germany
[3] GFZ German Research Centre for Geoscience, Telegrafenberg, 14473 Potsdam, Germany
[4] Geography Department, Humboldt-Universität zu Berlin, Unter den Linden 6, 10099 Berlin, Germany
[5] Integrative Research Institute on Transformations of Human-Environment Systems (IRI THESys), Humboldt Universität-zu-Berlin, Unter den Linden 6, 10099 Berlin, Germany

Correspondence to: Atabek Umirbekov (umirbekov@iamo.de)

Abstract. Due to the long memory of snow processes, statistical seasonal streamflow predictions in snow-dominated catchments typically rely on snowpack estimates. Using mountainous catchments in Central Asia as a case study, we demonstrate how seasonal hydrological forecasts benefit from incorporating large-scale climate oscillations (COs). First, we examine the teleconnections between the major COs and peak precipitation season in eight catchments across the Pamir and Tian-Shan mountains from February to June. We then employ a machine learning framework that incorporates snow water equivalent (SWE) and dominant COs indices as predictors for mean discharge from April to September. Our workflow leverages an ensemble technique that uses multiple SWE estimates from near-time global data sources and diverse types of explainable machine-learning models. We find that the winter states of the El Niño-Southern Oscillation and the North Atlantic Oscillation enhance SWE-based forecasts of seasonal discharge in the study catchments. We identify three instances in which the inclusion of COs as additional predictors could be instrumental for snowpack-based seasonal streamflow forecasting: 1) when forecasts are issued at extended lead times and accumulated SWE is not yet representative of seasonal terrestrial water storage; 2) when climate variability during the forecasted season plays a larger role in shaping seasonal discharge; and 3) SWE estimates for a catchment are subject to larger uncertainty. Our approach provides a novel way to reduce uncertainties in seasonal discharge predictions in data-scarce snowmelt-dominated catchments.

1. Introduction

Snowmelt-driven streamflow is a vital source of water supply for downstream regions around the globe, where it sustains ecosystems, agriculture, hydropower, and numerous other human activities (Immerzeel et al., 2020; Viviroli et al., 2007). It is estimated that around two billion of the world`s population lives in snow-sensitive basins (Mankin et al., 2015) and it is projected that around a quarter of world`s lowland population will be critically dependent on snow- and glacier-melt runoff from mountains by the middle of the century (Viviroli et al., 2020). Accurate water availability forecasts are essential for the sustainability and resilience of water-dependent human and ecological systems in these regions.

Seasonal streamflow forecasts are usually generated using either dynamic or statistical approaches. Dynamic forecasts encompass a hydrological or land-surface model to estimate current hydrologic conditions, typically with assimilation of observational data and climate forecasts to update and correct the resulting model state variables (Troin et al., 2021). One major advantage of dynamical approaches is the continuous production of future streamflow states (Modi et al., 2022). On the other hand, one of the main limitations of dynamical forecasts is their high computational demands and dependence on spatially distributed meteorological variables obtained from numerical climate models, which might be prone to uncertainties. Statistical approaches rely on the empirical relationship between one or multiple variables and seasonal streamflow. In this respect,

https://doi.org/10.5194/hess-2024-174
Preprint. Discussion started: 26 July 2024

Hydrology and Earth System Sciences
Discussions

statistical hydrological forecasts in the context of snow-dominated catchments offer advantages in terms of lower computational complexity and reliance primarily on initial hydrological conditions.

Because accumulated snowpack is a primary source of predictability of river streamflow in snowmelt-dominated basins (Pechlivanidis et al., 2020), statistical forecasts of seasonal streamflow often rely solely on accumulated snowpack. Emerging evidence suggests that statistical-based forecast techniques that leverage initial hydrological conditions and large-scale climate indices could improve skill compared to current forecast approaches (Mendoza et al., 2017; Lehner et al., 2018). Apart from cases when catchments are influenced by strong teleconnections with large-scale climate oscillations (Mendoza et al., 2017), it remains unclear under what other conditions combining snow with climate indices offers benefits.

Water is inextricably intertwined with the development challenges of Central Asia, yet its timely availability during vegetation season remains erratic. The hydrological discharge in Central Asian rivers is subject to large seasonal temperature and precipitation cycles; the latter falls as snow in winter, and its melting contributes to spring and summer runoff. The high variability of precipitation during the cold season thus eventually determines high interannual volatility of river streamflow in Central Asian endorheic rivers since most discharge originates from snowmelt in the Pamir and Tian Shan mountains (Viviroli & Weingartner, 2004). This high hydroclimatic variability subsequently underscores the need for improved water availability forecasting during the irrigation season (Xenarios et al., 2019).

Research on seasonal river discharge forecasting in Central Asia can be classified into two mainstream approaches. One approach explored the predictability of mean discharge during April-September (from now on referred to as 'vegetation season") by using estimates of terrestrial water storage that accumulates in mountain catchments throughout preceding November to March (from now on referred to as "cold season"). Terrestrial water storage in Central Asia is dominated by large annual cycles, with most precipitation during the extended cold season that lasts from autumn to spring and accumulates as snowpack in the mountain catchments. In the absence of in-situ snow water equivalent (SWE) data, several studies explored the use of proxies such as cumulative precipitation over the cold season (Dixon and Wilby, 2016; Schär et al., 2004), or satellite-derived snow cover derived from satellite, antecedent discharge, and other predictors (Apel et al., 2019; Gafurov et al., 2016).

Another approach uses climate indices of global climate oscillations as predictors, some of which are known to have a noticeable impact on hydroclimate variability in Central Asia. It was found that El Niño-Southern Oscillation (ENSO) during its warm phase (aka El-Niño) increases precipitation intensity in Central Asia, most pronounced from autumn to summer (Mariotti, 2007; Chen et al., 2018). In contrast, ENSO in its cold phase (i.e. La-Niña) is associated with below-average precipitation in the region. The Pacific Decadal Oscillation (PDO) can intensify ENSO's effects: during ENSO's La Niña phase, when the PDO is in its negative phase, Central Asia is more susceptible to severe droughts (Wang et al., 2014). The North Atlantic Oscillation (NAO), Scandinavian pattern (SCAN), and East Atlantic/Western Russia pattern (EAWR), all of which refer to periodic fluctuations in atmospheric pressure between specific regions of the Atlantic Ocean and Eurasia, are also known to affect hydroclimatic variability in Central Asia (Syed et al., 2010). Several studies previously showed that indices of these climate oscillations can be used for forecasting seasonal precipitation (Gerlitz et al., 2019; Umirbekov et al., 2022) and streamflow in the region (Barlow and Tippett, 2008; Dixon and Wilby, 2019).

Both approaches have strengths and weaknesses. Using terrestrial water storage estimates as predictors produces accurate seasonal runoff predictions, though their accuracy gradually degrades with extending lead times (Apel et al., 2018). In contrast, climate indices offer seasonal hydrological outlooks well before the start of the vegetation season, though at the cost of higher

https://doi.org/10.5194/hess-2024-174
Preprint. Discussion started: 26 July 2024

uncertainties. Combining the strengths of both approaches into a two-tiered approach was suggested for forecasting seasonal runoff (Gerlitz et al., 2020). Accordingly, early seasonal outlooks should employ large global oscillations to predict cold season precipitation anomalies. By the start of the vegetation season, seasonal hydrological projections should rely more on the abovementioned proxies of seasonal water storage. However, a common approach to seasonal hydrological forecasting typically builds on two main elements: initial hydrological conditions and future climate variability (WMO, 2021). From this perspective, combining the main predictors the two approaches rely on could be more appropriate: so that the accumulated catchment snowpack represents the initial hydrological conditions, and climate oscillation indices serve as precursors to climate variability during the targeted season.

Another challenge hampering the development of advanced forecasting techniques in the region is a scarcity of in-situ meteorological observations, particularly for snow mass measurements. In the past, local hydrometeorological agencies used to conduct snow depth measurements across the region's main catchments. This practice was discontinued mainly due to the underfinancing of the relevant agencies that persisted for the past three decades (Xenarios et al., 2019). Satellite or reanalysis datasets available in near-real time can be an alternative source for estimating SWE. Still, they might be prone to inherent uncertainties and insufficient spatial resolution to capture variations of accumulated SWE in complex terrain. A promising option to reduce uncertainty in modelled products is to apply an ensemble technique instead of relying on a single model estimate (Murray, 2018; Zounemat-Kermani et al., 2021).

This paper aims to introduce and test a new framework for statistical forecasts of seasonal river discharge in snow-dominated catchments by coupling estimates of snow water equivalent with climate oscillation indices that condition hydroclimatic variability in the upcoming season. Our approach relies on an ensemble of diverse estimates of catchment-averaged SWE derived or simulated using multiple global reanalysis products supplemented with climate indices that affect hydroclimatic variability across Central Asia. We used generalized linear regression and machine learning techniques, such as Random Forest, Gaussian Process, and Support Vector Regression, which produce a range of individual forecasts. Finally, we employ an ensemble stacking approach, a type of ensemble learning that uses the forecasts from individual models as inputs to a model that produces a more reliable final prediction.

2. Study Area

The study area encompasses eight diverse snowmelt-dominated catchments in the Pamir, Hindukush, and Tian-Shan mountains (Figure 1, Table 1). The size of the selected catchments varies from 343 to 296,000 km2, and the mean catchment altitude ranges from 1,700 to 3,500 meters. The catchments include the largest rivers in the region, the Amudarya and Naryn (the main tributary of the Syrdarya), which embed several smaller tributary sub-catchments.

Table 1. Major geographical and climatic characteristics of the study catchments

	Catchment	Gauging station name	Station location (lat, lon)	Catchment area (km^2)	Catchment mean altitude (m.a.s.l)	Mean seasonal discharge Apr-Sep (m^3/sec)	Mean annual precipitation (mm)
1	Murghab	Takhta Bazar	35.96, 62.91	35,582	1,710	41	320
2	Amudarya	Kerki	37.84, 65.23	296,300	2,550	1,876	380

https://doi.org/10.5194/hess-2024-174
Preprint. Discussion started: 26 July 2024

Hydrology and Earth System Sciences
Discussions
Open Access
EGU

	Catchment	Gauging station name	Station location (lat, lon)	Catchment area (km^2)	Catchment mean altitude (m.a.s.l)	Mean seasonal discharge Apr-Sep (m^3/sec)	Mean annual precipitation (mm)
3	Varzob	Dagana	38.70, 68.79	1,279	2,700	79	654
4	Vaksh	Komsomolabad	38.86, 69.94	28,908	3,530	996	530
5	Kashkadarya	Varganza	40.81, 73.26	343	2,663	18	530
6	Zarafshan	Dupuli	39.49, 67.80	10,310	3,125	243	516
7	Naryn	Toktogul	41.77, 73.29	46,667	2,940	561	392
8	Chu	Kochkor	42.25, 75.83	5,305	2,934	35	391

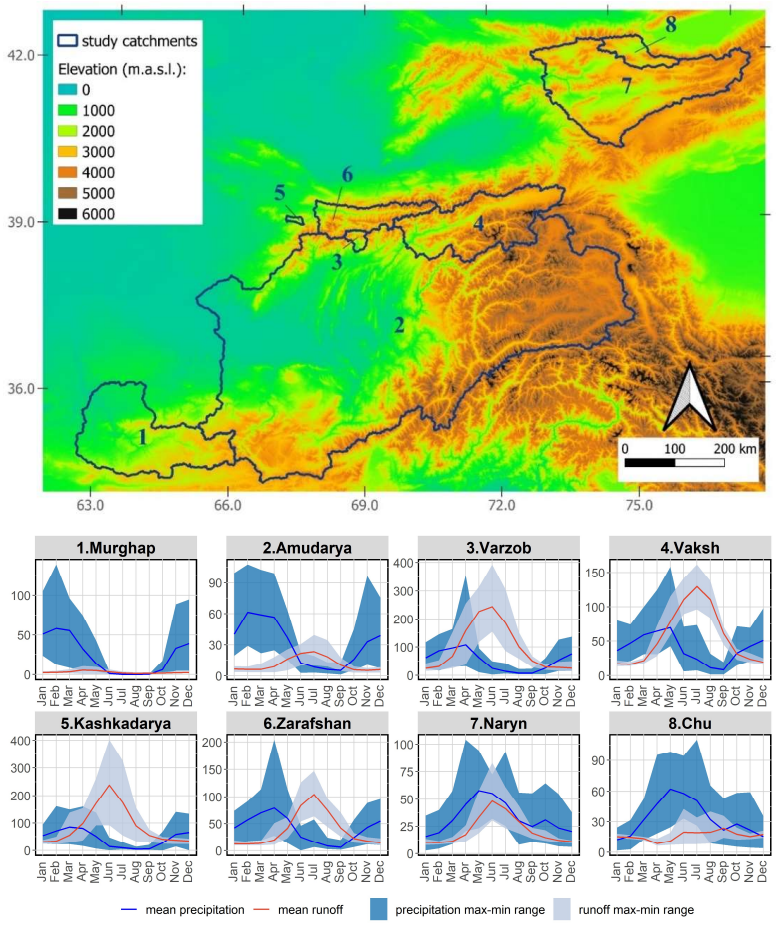

120

https://doi.org/10.5194/hess-2024-174
Preprint. Discussion started: 26 July 2024

Hydrology and Earth System Sciences
Discussions

Figure 1. Location of the study catchments (upper map), monthly means and ranges for precipitation and runoff in mm (bottom graphs)

3. Data

The predictant variable represents seasonal discharge, calculated as the mean discharge from April to September. We obtained monthly discharge data for the study catchments from 2000 to 2018 from hydrometeorological agencies in Central Asian countries. We aggregated these into mean discharge from April to September, resulting in approximately eighteen observations of seasonal discharge for each catchment.

As the primary predictor variable, we use four basin-averaged SWE estimates that can be derived from near-real time global climate datasets available in near real time (Table 2). These include two SWE estimates from global and regional reanalysis datasets, i.e. ERA5-Land (Muñoz-Sabater et al., 2021) and Land Data Assimilation System Central Asia (McNally et al., 2022). In addition, we simulated two SWE estimates using the GEMS snow model (Umirbekov et al., 2023) forced by global precipitation and temperature data available in near-real time. One simulated SWE time series is obtained by forcing the snow model with the Multi-Source Weather dataset, which is generated by bias-correcting and downscaling ERA5 (Beck et al., 2021). The fourth SWE estimate is simulated using precipitation estimates from the Integrated Multi-satellite Retrievals GPM IMERG (Huffman et al., 2019) and temperature estimates from MSWX. We used a 'Late Run' version of GPM IMERG precipitation estimates, accessible in near-real time albeit lacking adjustments using ground precipitation data as in the 'Final' product, which becomes available two months later.

Candidates for additional predictors include the monthly indices of the El Niño–-Southern Oscillation (ENSO), the Pacific Decadal Oscillation (PDO), the North Atlantic Oscillation (NAO) and the Scandinavian Pattern (SCAN).

Table 2. Snow water equivalent estimates and climate oscillation indices that were used as predictors in this study

Type	Predictor (abbreviation)	Description	Source
Snow Water Equivalent estimates	ERA5-L	Retrieved from the ERA5-Land reanalysis dataset	Muñoz-Sabater et al., 2021
	FLDAS	Retrieved from the Land Data Assimilation System Central Asia	McNally et al., 2022
	MSWX	Simulated using GEMS model forced by precipitation and temperature estimates from Multi-Source Weather dataset	Beck et al., 2021
	GPM	Simulated using GEMS model forced by precipitation from GPM IMERG and temperature from MSWX datasets	Huffman et al., 2019
Climate Oscillation Indices	SOI	Southern Oscillation Index	Ropelewski and Jones 1987
	PDO	Pacific Decadal Oscillation	Mantua *et al* 1997
	EAWR	East Atlantic/West Russia pattern (EAWR)	Barnston and Livezey 1987

https://doi.org/10.5194/hess-2024-174
Preprint. Discussion started: 26 July 2024

Hydrology and Earth System Sciences
Discussions

NAO	North Atlantic Oscillation (NAO)	Barnston and Livezey 1987
SCAN	Scandinavian pattern	Barnston and Livezey 1987

4. Methods

4.1 Determining associations between climate oscillations and hydroclimatic variability across study catchments

To determine linkages between the selected climate oscillations and hydroclimatic variability across the catchments, we calculated Spearman's rank correlations with precipitation during months with higher magnitude and interannual variability. We used the CHELSA-W5E5 precipitation dataset (Karger et al., 2022) to construct catchment-averaged precipitation time series from 1979 to 2016. The annual precipitation cycle in the studied catchments exhibits two distinct sub-regional patterns (see Figure 1). Catchments in the Pamir and western Tian-Shan experience increasing precipitation during winter, peaking in the spring, and decreasing during summer. In contrast, the Naryn and Chu catchments, located in the interior and northern Tian-Shan, receive most precipitation from late spring to early summer and less precipitation in winter. Across all catchments, the interannual variability is greatest during the months with the highest precipitation totals. We have defined the common peak precipitation season for the region as February to June, since this period covers the months with the highest precipitation levels and the greatest interannual variability across all the studied catchments.We then calculated Spearman's rank correlation coefficient between the catchment averaged precipitation for February-July (referred to here as ‘peak precipitation season’) and each climate oscillation index at varied lead-lag times. To identify when oscillations show the strongest association with the precipitation season, we calculated the correlation for each oscillation index from August of the preceding year to July, the final month of the peak precipitation season.In addition, we calculated correlations between the climate indices and mean discharge during the vegetation season using the same procedure.

4.2 Stacked ensemble-based prediction of seasonal discharge

Our forecast modelling framework employs an ensemble stacking approach with four main steps (Figure 2). In the first stage, we combine each basin-averaged SWE estimate with climate oscillation indices at months when they exhibit higher association with in-season precipitation peaks. Four different SWE products result in four datasets with varying SWE estimates but the same set of selected climate oscillation indices for each catchment.

https://doi.org/10.5194/hess-2024-174
Preprint. Discussion started: 26 July 2024

Hydrology and Earth System Sciences
Discussions

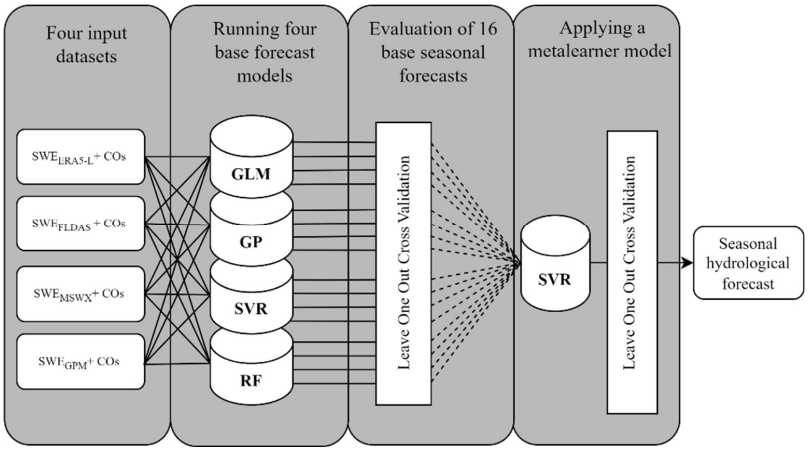

Figure 2. Workflow of the ensemble-based forecast approach

We then use four different forecast models (from now on referred to as "*base models*"), each forced with the four input datasets to produce a range of 16 seasonal forecasts. The four base models are comprised of the generalized linear model (GLM), gaussian process regression with the linear kernel (GP), support vector regression with the linear kernel (SVR) and random forest (RF). The latter two model algorithms have parameters that control internal model complexity. For example, the "*cost"* parameter in SVR limits training errors against maximizing the margin of the decision function, and "*mtry"* in RF determines the number of predictors that can be taken into account at each split point of a single tree. We set these parameters to relatively lower levels (cost=0.3 in the case of SVR and mtry=2 in the case of RF), which helps to avoid overfitting and facilitates a higher degree of generalizability.

In the next step, we evaluate each of the 16 base model predictions using leave-one-out cross-validation (LOOCV). Rather than using all 16 base model forecasts in subsequent steps, we apply a threshold that filters out weaker predictions. This threshold requires a leave-one-out cross-validated R-squared coefficient of base model performance to be greater than 0.2 to be considered for further analysis. This threshold was optimal during LOOCV regarding predictive performance for the stacking ensemble.

In the final step, those base model predictions that pass the LOOCV test become inputs for a final forecast model (from now on called "*ensemble model*"). Since all selected base model predictions would exhibit some degree of correlation among themselves, we employ the SVR algorithm as a meta-learner model, which is known to be less sensitive to multicollinearity (Farrell et al., 2019). The final prediction of the meta-learner model is again assessed using LOOCV. Finally, we validate the resulting model using a few observations of seasonal discharge, which were held out during the training of the models.

We apply the procedures described above for each standard forecast issue time adopted by hydrological agencies in Central Asia, starting from January 1st, that is a three-month lead time concerning the April-September season, and ending with the final forecast issued just before the start of the season, i.e., on April 1st. Each forecast uses inputs that are accessible by its issue date. For example, three-month lead forecasts can only use estimates of catchment SWE by January 1st and state of climate oscillations in previous months. To attain parsimonious forecast models, rather than incorporating all studied climate oscillation indices into a set of predictors, we followed a stepwise approach: each of the climate indices was added one at a time to the predictors set, which was then evaluated. This approach led to a final predictor set with the minimal combination necessary to produce plausible predictions for each catchment and each forecast issue date.

https://doi.org/10.5194/hess-2024-174
Preprint. Discussion started: 26 July 2024

Hydrology and Earth System Sciences
Discussions

4.3 Determination of supplementary importance of incorporating climate oscillations as additional predictors

We implement two track evaluation analyses to determine the value of adding COs as additional predictors into snow-based forecasts. First, we elaborate forecast models that assimilate only SWE estimates, using the same approach described in the previous section, and compare their performance with those that assimilate SWE and COs. Second, we determine the relative importance of COs using the *feature importance ranking measure* method (Greenwell et al., 2018), which quantifies how much each input variable influences the predictions made by the model. The method assesses the impact of each input variable by estimating partial dependence plots (Friedman, 2001) and assigning higher (lower) importance rank to features that exhibit a steeper (flatter) partial dependence effect.

5. Results

5.1 Evaluation of SWE estimates

Figure *3.* Pearson`s correlation coefficients between the SWE estimates and mean seasonal discharge between April and September at different forecast lead months. The red line is the median across all snow products. Figure 3 summarizes the correlation coefficients between catchment-averaged SWE at different forecast issue dates and mean discharge during the vegetation season. The SWE estimates obtained from global reanalysis and satellite data exhibit varied degrees of connection with the seasonal discharge. For all catchments, the correlation in general tends to increase with shorter lead times, i.e., with SWE estimates for January 1st having the lowest correlation and those for April 1st having the highest. There is no discernible best-performing product across the four SWE estimates overall, with some products better performing in one catchment but underperforming in another. Nevertheless, SWE estimates based on ERA5-L and MSWX generally show a higher correlation with seasonal discharge across most catchments.

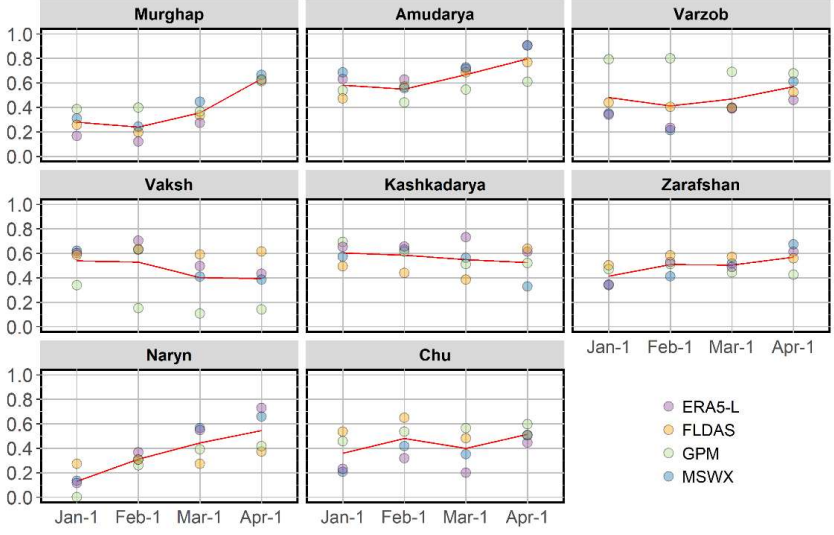

Figure 3. Pearson`s correlation coefficients between the SWE estimates and mean seasonal discharge between April and September at different forecast lead months. The red line is the median across all snow products.

5.2 Association between climate oscillations and hydroclimatic variability across the study catchments

https://doi.org/10.5194/hess-2024-174
Preprint. Discussion started: 26 July 2024

Evaluation of the climate oscillation indices revealed diverse associations with peak season precipitation and mean river discharge during the vegetation season across the catchments (Figure 4, upper graph). In all catchments, the February-July precipitation exhibits a robust and persistent association with ENSO, represented by the Southern Oscillation Index (SOI) and the Pacific Decadal Oscillation (PDO), over an extended timeframe compared to other oscillations. There is a significant negative correlation between peak precipitation season and SOI in all catchments, evident three months before the season's commencement. This relationship persists for a longer duration compared to any other climate oscillation. On the other hand, PDO exhibits a positive link with seasonal precipitation, becoming noticeable as early as four months before the season's onset and reaching its most substantial level in November.

Like ENSO and PDO, the East Atlantic/West Russia pattern (EAWR) consistently demonstrates a stronger correlation across most catchments before the peak precipitation season. Notably, the October state of EAWR shows a substantial positive correlation with peak precipitation across all catchments; however, it becomes more variable as the season progresses.

On the other hand, the North Atlantic Oscillation (NAO) and the Scandinavian Pattern (SCAN) show a relatively less pronounced association with the peak precipitation season, with correlations that vary depending on the lead time. From December to March, the NAO shows a weak but persistent negative relationship with the peak precipitation season in most catchments. In January, at the beginning of the peak precipitation season, a considerable portion of the catchments demonstrates a negative correlation with the state of SCAN. However, as the season progresses and reaches March, there is a noticeable shift, with all catchments showing a stronger and positive correlation with the state of SCAN.

The correlation between the climate indices and mean river discharge during April-September exhibits almost the same pattern (Figure 4, bottom graph), which implies that discharge variability is predominantly driven by precipitation that falls during February-July.

https://doi.org/10.5194/hess-2024-174
Preprint. Discussion started: 26 July 2024

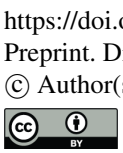

Hydrology and Earth System Sciences
Discussions
Open Access
EGU

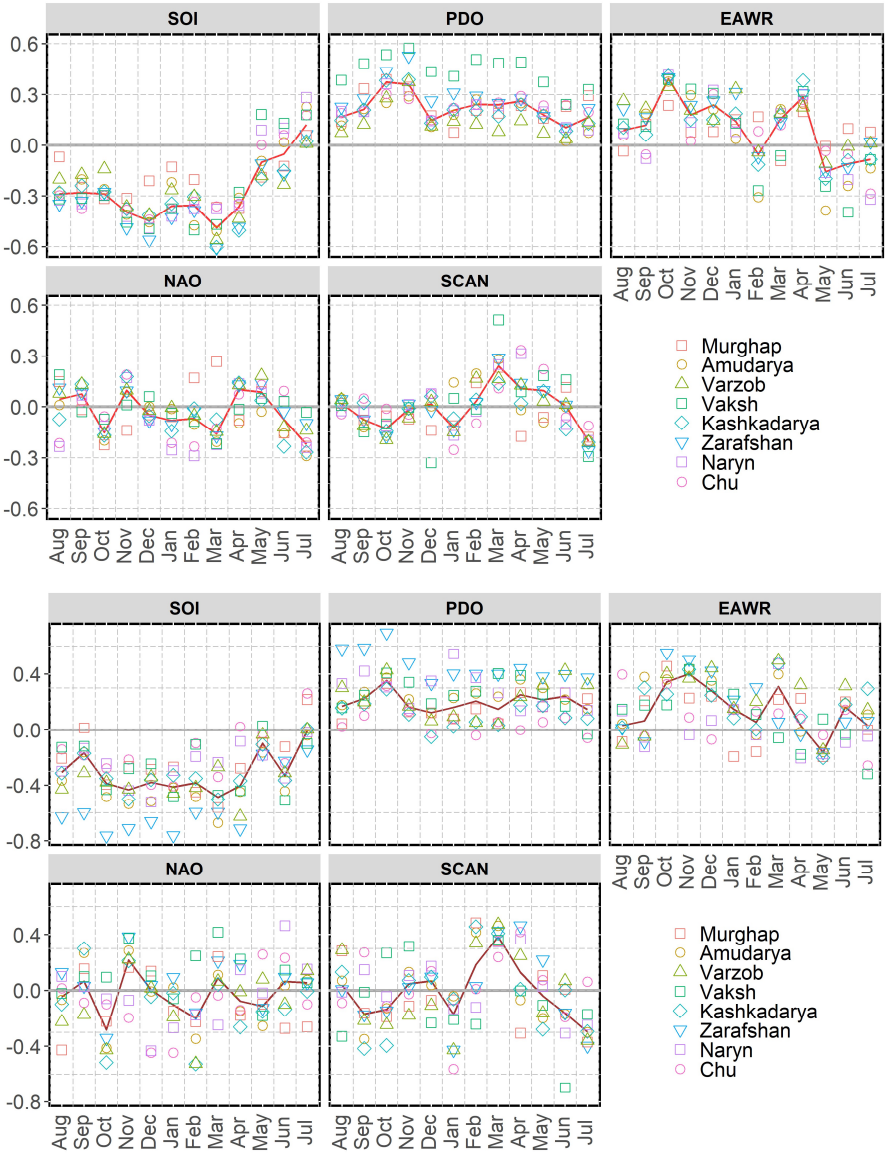

255 **Figure 4. Spearman's rank correlation coefficients between the climate oscillation indices and precipitation from February to July precipitation (top) and mean seasonal discharge from April to September (bottom).** The X-axis denotes months of a climate index. The red line represents a median for correlation coefficients across all catchments in each month.

5.3 Performance of seasonal discharge forecasts

260 Figure 5 below summarizes a set of final predictors per studied catchment, obtained after screening COs associations with peak precipitation and mean discharge during vegetation season and following a stepwise selection procedure using the ensemble-stacking forecast approach described in section 4.2.

While the input dataset for the base models included SWE estimates, the combination of climate oscillations they rely on varies
265 depending on a catchment location and elevation. In most catchments, the base models incorporated the late autumn state of PDO or the December state of SOI. While SOI appears equally crucial in most catchments, PDO generally persisted in

https://doi.org/10.5194/hess-2024-174
Preprint. Discussion started: 26 July 2024

Hydrology and Earth System Sciences
Discussions

catchments located in Pamir and west Tian-Shan. The winter state of NAO and SCAN are another source of predictability in many of the catchments but have variable temporal signatures. In the case of the Murghap, where workable base models were obtained only for the April 1st forecast, they rely solely on SWE estimates and do not include any of the climate oscillations as predictors.

Selected NAO or SCAN predictors tend to have the same temporal lags for neighbouring catchments. For instance, the Naryn and Chu catchments in the Tian-Shan, which have similar seasonal precipitation patterns, use the NAO condition in December as one of their predictors. The Varzob and Vaksh rivers, which are high-elevation tributaries of the Amudarya, use the January state of SCAN, while the latter becomes a more robust forecast for the larger Amudarya watershed only one month later, in February.

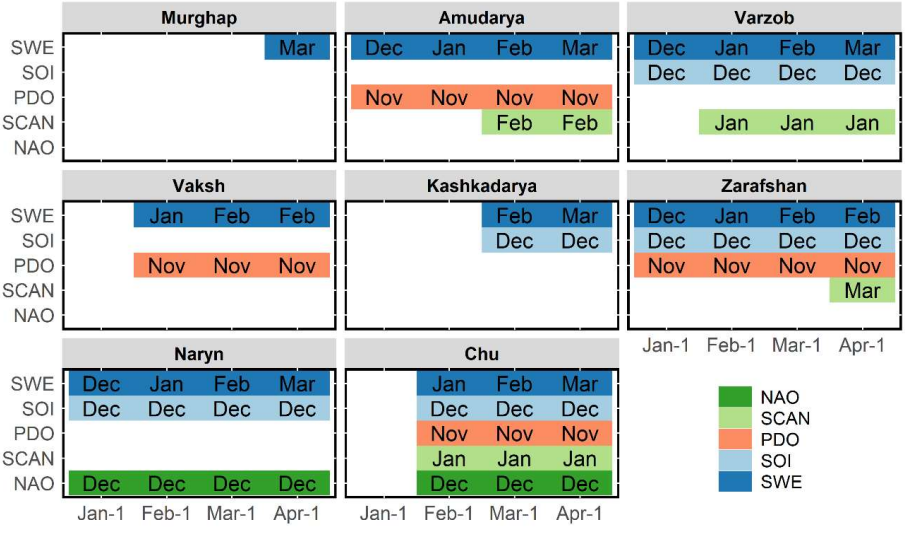

Figure 5. Predictors at different forecast issue times. Abbreviations within boxes indicate the month of the respective climate oscillation index or catchment-averaged SWE used as predictors. For example, the April 1st forecast models for the Amudarya river use as predictors the SWE estimate as of the end of March, the state of the PDO index in November, and the SCAN index in February.

The ensemble-based forecasting framework plausibly simulated seasonal discharge across all catchments, albeit with varying temporal performance based on lead time (Figure 6). The ensemble model's LOOCV R-squared coefficient ranges between 0.3 and 0.5 for the extended lead time forecast (1 January) but gradually increases with decreasing lead time, reaching 0.8 and 0.9 for the April 1 forecast. The performance of the meta-learner model depends on the number and diversity of the resultant individual base models and is typically superior to those of the latter.

Fewer base models appear capable of predicting seasonal discharge at longer lead times, resulting in a relatively lower performance of the meta-learner model on the January 1st forecast. For the Murghab, Kashkadarya, and Chu catchments, no feasible base models were obtained for the January 1st forecast. Furthermore, workable base models and the derived meta-learner model for Murghap are only obtainable for the April 1st forecast.

There are no discernible winners in terms of performance of the base model types across lead times, especially for the final (April 1st) forecast. However, the base models' performance has some distinct spatial heterogeneity, depending on which SWE

https://doi.org/10.5194/hess-2024-174
Preprint. Discussion started: 26 July 2024

Hydrology and Earth System Sciences
Discussions

product they assimilate. For example, all base models for the Kashkadarya retained after cross-validation rely only on $SWE_{ERA5\text{-}L}$ or SWE_{MSWX} as inputs. In contrast, all base models obtained for the Vaksh catchment rely only on SWE_{FLDAS} and SWE_{GPM}. The seasonal discharge in the largest catchments, such as Amudarya and Naryn, is also better explained by base models that use $SWE_{ERA5\text{-}L}$ or SWE_{MSWX}.

The results suggest that models incorporating GPM IMERG have higher uncertainty, reflected in overall lower cross-validation performance, except in the highly elevated Varzob and Zarafshan catchments. This is likely due to the lower accuracy of the GPM IMERG`s Late Run product, which includes only climatological adjustment. In contrast, its final product ("Final Run") comes with adjustments using gauge data. However, the latter is only available at a three-month latency time, precluding its operational forecasting use.

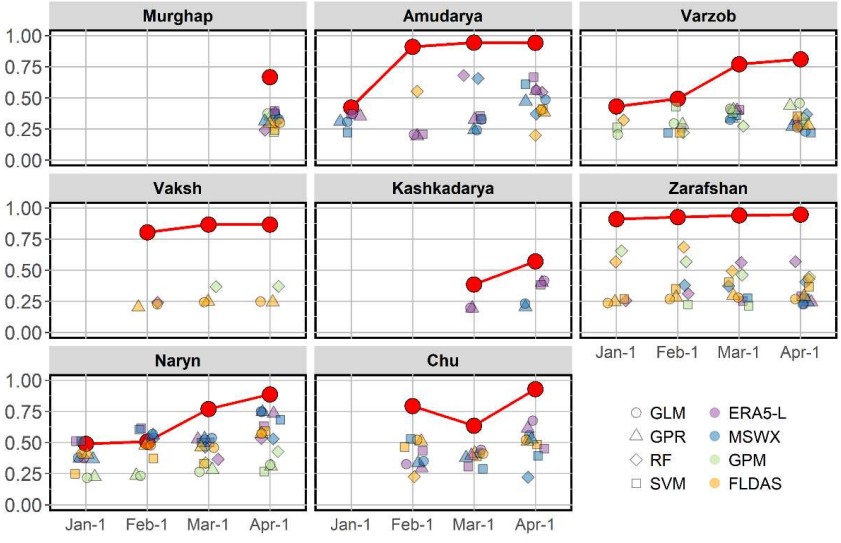

Figure 6. Resulted LOOCV R-squared coefficients of individual base models at different lead months and the LOOCV R-squared of the meta-learner model (red line).

The performance of the meta-learner model also yielded comparable results for both LOOCV validation and hold-out test set in terms of normalized Mean Absolute Error (Figure 7, upper graph). The normalized MAEs follow the same temporal pattern as the R-squared coefficient, with relatively larger errors for early forecasts that gradually decrease with decreasing lead times. Due to a limited number of discharge observations, the hold-out included only three last observations for seasonal discharge (which even became two in the case of the Naryn and Zarafshan catchments). In many instances, the hold-out set across the catchments contained a diverse combination of high and low observed seasonal discharge, which were plausibly predicted by the final meta-learner model (Figure 8). For the Kashkadrya and Chu rivers, the model correctly predicted the lowest observed seasonal discharges over the entire observation period, which were in the hold-out set. Similarly, the final meta-learner model coherently reproduced lower discharges from hold-out sets in the Amudarya andNaryn rivers below the 25th quantile of all observation years.

Figure 7 (bottom graph) also compares the performance of the forecast models based only on SWE estimates. SWE-only forecasts have larger uncertainties, with higher MAE errors for the LOOCV validation, especially the hold-out test set. The mean absolute errors also tend to be larger at shorter lead times, which may imply higher uncertainties in SWE estimates

https://doi.org/10.5194/hess-2024-174
Preprint. Discussion started: 26 July 2024

Hydrology and Earth System Sciences
Discussions
Open Access
EGU

325 during the snow-melt phase. In addition in certain catchments, we could not develop effective meta-learner models for extended lead times.

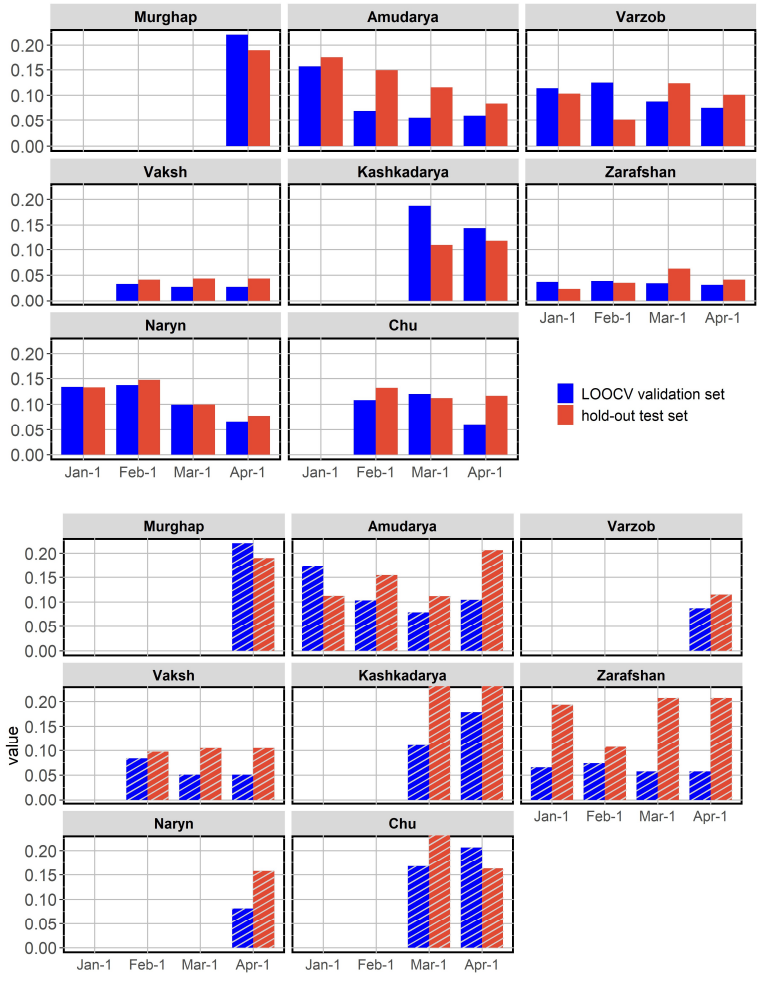

330 **Figure 7. Normalized MAE of the simulated seasonal discharge by ensemble models for training and hold-out sets at different forecast lead months, including SWE and climate oscillation indices (upper) and only SWE (bottom) as predictors.**

https://doi.org/10.5194/hess-2024-174
Preprint. Discussion started: 26 July 2024

Hydrology and Earth System Sciences
Discussions
Open Access
EGU

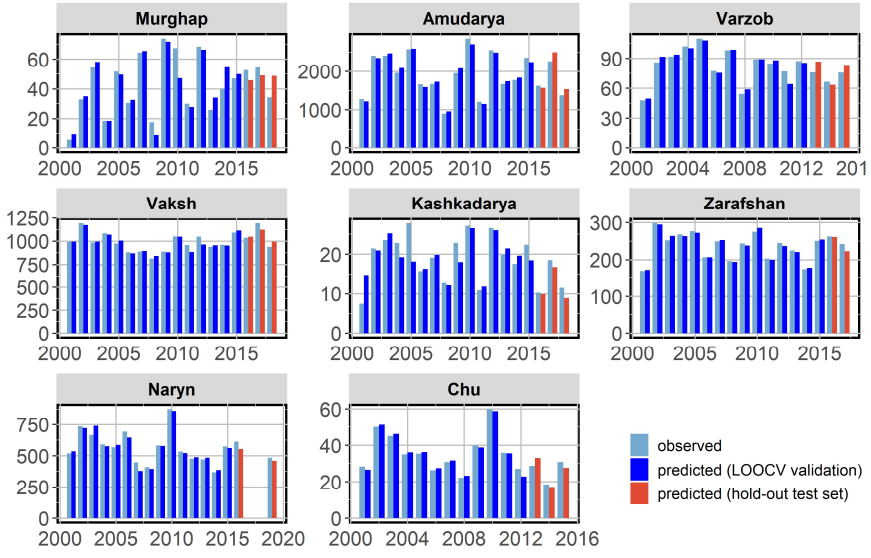

Figure 8. Observed vs simulated seasonal discharge using Apr 1st forecast ensemble model

335

5.4 Importance of climate oscillation indices as predictors

The importance of predictors varies depending on the catchment location and the forecast issue date (Figure 9). Regardless of the forecast issue date, SWE is a major predictor in most catchments located in Pamir, and its significance generally arises with decreasing lead times. Its incremental value is evident in the basins in the western part of the study area, the Pamir
340 Mountains. Nevertheless, the supplementary predictive value of COs is visible in all basins regardless of their location except for Murghap, where forecast models rely only on SWE estimates. The predictive power of COs is highest for the two catchments located in the inner and northern Tian-Shan, Naryn and Chu. Especially in Chu, the COs contribute to more than half of the predictive power of the forecast models across all forecast issue dates.

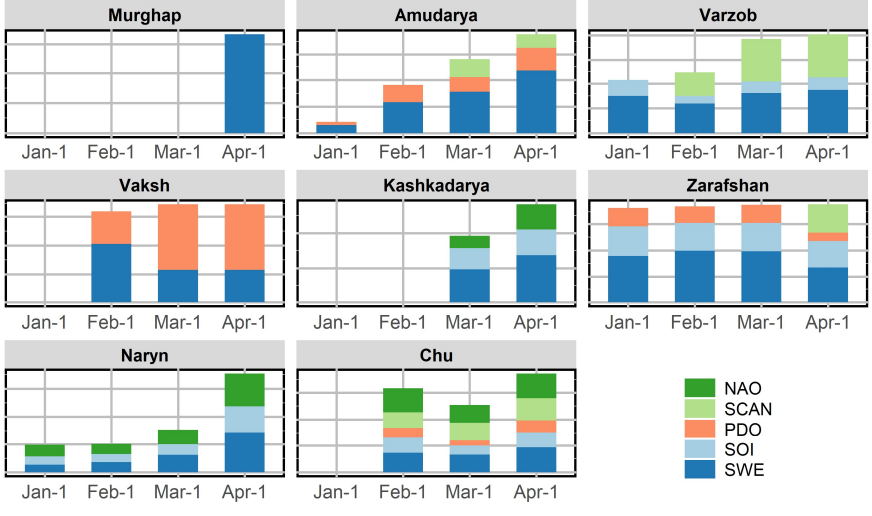

345

Figure 9. The relative importance of predictors at different forecast issue dates

https://doi.org/10.5194/hess-2024-174
Preprint. Discussion started: 26 July 2024

Hydrology and Earth System Sciences
Discussions

6. Summary and Discussion

Our findings suggest that near real-time SWE estimates can be effectively derived from global reanalysis or satellite data. Still, they are subject to spatial bias and uncertainty, which may be due to uncertainties in underlying precipitation and temperature inputs. The uncertainties in the SWE estimates may propagate across time and enlarge during the snow ablation phase. Assimilating SWE data from multiple global sources helps mitigate these biases, and predictions that pass cross-validation filters reflect the accuracy of SWE products specific to catchment locations. Nevertheless, although catchment-averaged SWE estimates improve with the assimilation of multiple snow products, they may still tend to contain spatial uncertainties that increase during the ablation phase.

Multiple global ocean-atmospheric oscillations modulate the seasonal hydroclimatic patterns in the Pamir and Tian-Shan mountains, each with different temporal effects. The findings suggest that the magnitude of both seasonal precipitation and discharge is associated with the late autumn to winter state of ENSO (approximated in our study with SOI). PDO is known to mimic ENSO-like variability on monthly scales and has a pronounced impact on the interdecadal scale. This could explain the similarity in dominant lead times observed in our analysis with SOI. Late winter to spring states of NAO and SCAN contribute to hydroclimatic predictability in many studied catchments, mainly showing higher significance in the Tian-Shan domain. All these spatial and temporal patterns are broadly consistent with several earlier findings (e.g., Mariotti 2007, Wang et al. 2014, Dixon and Wilby 2019, Gerlitz et al. 2019).

The associations between the climate indices with both precipitation and discharge exhibit an almost identical pattern, implying that river discharge's interannual volatility from April to September is substantially driven by the peak precipitation period, which we determine as February to July. This implies that SWE accumulated by the middle of winter is a weak precursor of hydrologic variability in the upcoming season, which our findings assert. On the other hand, this serves as an argument for using climate oscillation indices beside the catchment snowpack in discharge forecasts at extended lead times. Following the traditional approach towards seasonal hydrological predictions, SWE estimates initial hydrological conditions and climate oscillation indices as a proxy of climate variability during the target season.

Our experiment, which combines snow and climate indices as predictors, confirms this assumption. The resulting forecast models generate credible simulations of seasonal discharge across all studied catchments, albeit with performance variations depending on lead time. The forecast models incorporating both SWE and COs perform better than the SWE-only models, evidenced by lower forecast uncertainties and minor errors in LOOCV validation and hold-out test sets. Due to a limited number of observations, our evaluation only included a small set of the most recent discharge data for some rivers. Despite this limitation, the meta-learner models accurately predicted high and low seasonal discharge values in the hold-out set for some catchments, showcasing its effectiveness in predicting hydrological extremes on seasonal scales.

The resulting forecast models underscore the significance of SWE as one of the primary predictors in most catchments in the Pamir region, with its importance becoming more pronounced during the peak SWE period, typically occurring in mid-spring.Nevertheless, the forecast models also gain valuable predictive power from climate oscillation indices during extended and shorter lead times. The importance of specific climate oscillations as predictors varied across catchments. In most catchments, the SOI, PDO, or both were utilized, indicating the dominant influence of ENSO phenomena. Moreover, the results suggest that the NAO and SCAN exhibit a relatively higher predictive power for catchments in the Tian-Shan region.

The predictive importance of climate oscillations equalled or exceeded that of SWE in the Naryn and Chu catchments located in Tian-Shan, as well as in high-elevated catchments in Pamir, such as Zarafshan, Varzob, and Vaksh. The former might be

https://doi.org/10.5194/hess-2024-174
Preprint. Discussion started: 26 July 2024

390 explained by a distinctive precipitation cycle across Tian-Shan, which peaks during summer, i.e., considerably later than the final forecast issue date (April 1st). Consequently, SWE estimates have comparably smaller power to capture upcoming hydroclimatic variability than other catchments where precipitation peaking occurs during spring months and thus is embedded in SWE estimates by April 1st. This is better exemplified by the forecast model for the Murghap catchment, which doesn't integrate any climate oscillations, likely due to the majority of seasonal precipitation occurring before spring.The higher
395 predictive power of the oscillations for high-elevated catchments may be attributed to the poorer performance of the satellites and reanalyses of precipitation estimates over high elevations in the region (Peña-Guerrero et al., 2022), which subsequently propagate as uncertainties in the SWE estimates. In this regard, the higher predictive performance of climate oscillation indices across those catchments is assumingly reasoned by their compensation for uncertainties in SWE estimates.

400 Based on the abovementioned, we identify three specific cases when the incorporation of COs as additional predictors helps to improve seasonal discharge forecasts in snow-dominated catchments:

1) *Extended lead time forecasts with early seasonal SWE*: When seasonal discharge forecasts are made well in advance, but SWE is not a reliable representation of seasonal terrestrial water storage, climate oscillations may provide additional insights into anticipated hydroclimatic conditions.

405 2) *Dominant climate variability regime during the target season:* When the seasonal discharge is more influenced by in-season climate variability than by accumulated SWE before the season, climate oscillations can serve as adequate proxies for this variability.

3) *Uncertainties in catchment SWE estimates:* High uncertainties in SWE estimates for a particular catchment result in higher errors in discharge predictions. These uncertainties can be partially compensated by leveraging the forecasts with
410 climate oscillations, leading to more reliable seasonal discharge predictions.

In-situ observations of essential climate variables, such as snowpack properties, are scarce in Global South, especially mountainous regions, impeding hydrological forecasting. Previous research has demonstrated how, in the absence of in-situ snow observations, satellite-derived snow cover, precipitation and temperature can serve as proxies of terrestrial water storage
415 and improve seasonal discharge forecasting in Central Asia (Apel et al., 2018; Gafurov et al., 2016). Additionally, other studies have investigated how climate indices characterize hydroclimatic variability in the region over longer lead times (Dixon and Wilby, 2019). By combining the strengths of these two approaches, our modelling framework offers a new way to make hydrological predictions in the region. It leverages an ensemble technique that uses multiple estimates from global data, a diverse set of more straightforward types of machine learning methods with loose tuning parameters. These elements allow us
420 to achieve reliable forecast models even when in-situ discharge observations are short.

Code and Data Availability

R script to reproduce results in this paper is available at Zenodo (Umirbekov et al., 2024), under the Creative Commons Attribution CC BY 4.0 International license. The same record contains related data files, including: mean seasonal discharge of the studied catchment, gridded daily SWE data for the study area, and, monthly indices of the climate oscillations.

425 **Author contributions**

AU and DM designed the study. All authors evaluated the findings and contributed to the interpretation of results. All authors contributed to writing and reviewing the manuscript. DM supervised the project.

https://doi.org/10.5194/hess-2024-174
Preprint. Discussion started: 26 July 2024

Competing interests

The contact author has declared that none of the authors has any competing interests.

Acknowledgements

This research has been supported by the Volkswagen Foundation (grant no. 96 264). We extend our sincere appreciation to the open-source developer community and individuals behind numerous R packages, including but not limited to caret (Kuhn, 2008), terra (Hijmans, 2023), vip (Greenwell and Boehmke, 2020), and dplyr (Wickham et al., 2023).

References

Apel, H., Abdykerimova, Z., Agalhanova, M., Baimaganbetov, A., Gavrilenko, N., Gerlitz, L., Kalashnikova, O., Unger-Shayesteh, K., Vorogushyn, S., and Gafurov, A.: Statistical forecast of seasonal discharge in Central Asia using observational records: development of a generic linear modelling tool for operational water resource management, Hydrol. Earth Syst. Sci., 22, 2225–2254, https://doi.org/10.5194/hess-22-2225-2018, 2018.

Aralova, D., Toderich, K., Jarihani, B., Gafurov, D., and Gismatulina, L.: Monitoring of vegetation condition using the NDVI/ENSO anomalies in Central Asia and their relationships with ONI (very strong) phases, in: Earth Resources and Environmental Remote Sensing/GIS Applications VII, 1000512, https://doi.org/10.1117/12.2242164, 2016.

Barlow, M. A. and Tippett, M. K.: Variability and Predictability of Central Asia River Flows: Antecedent Winter Precipitation and Large-Scale Teleconnections, J. Hydrometeorol., 9, 1334–1349, https://doi.org/10.1175/2008jhm976.1, 2008.

Barnston, A. G. and Livezey, R. E.: Classification, Seasonality and Persistence of Low-Frequency Atmospheric Circulation Patterns, Mon. Weather Rev., 115, 1083–1126, https://doi.org/10.1175/1520-0493(1987)115<1083:CSAPOL>2.0.CO;2, 1987.

Beck, H. E., van Dijk, A. I. J. M., Larraondo, P. R., McVicar, T. R., Pan, M., Dutra, E., and Miralles, D. G.: MSWX: global 3-hourly 0.1° bias-corrected meteorological data including near real-time updates and forecast ensembles, Bull. Am. Meteorol. Soc., 1–55, https://doi.org/10.1175/bams-d-21-0145.1, 2021.

Chen, X., Wang, S., Hu, Z., Zhou, Q., and Hu, Q.: Spatiotemporal characteristics of seasonal precipitation and their relationships with ENSO in Central Asia during 1901–2013, J. Geogr. Sci., 28, 1341–1368, https://doi.org/10.1007/s11442-018-1529-2, 2018.

Dixon, S. G. and Wilby, R. L.: Forecasting reservoir inflows using remotely sensed precipitation estimates: a pilot study for the River Naryn, Kyrgyzstan, Hydrol. Sci. J., 61, 107–122, https://doi.org/10.1080/02626667.2015.1006227, 2016.

Dixon, S. G. and Wilby, R. L.: A seasonal forecasting procedure for reservoir inflows in Central Asia, River Res. Appl., 35, 1141–1154, https://doi.org/10.1002/rra.3506, 2019.

Farrell, A., Wang, G., Rush, S. A., Martin, J. A., Belant, J. L., Butler, A. B., and Godwin, D.: Machine learning of large-scale spatial distributions of wild turkeys with high-dimensional environmental data, Ecol. Evol., 9, 5938–5949, https://doi.org/10.1002/ece3.5177, 2019.

Gafurov, A., Lüdtke, S., Unger-Shayesteh, K., Vorogushyn, S., Schöne, T., Schmidt, S., Kalashnikova, O., and Merz, B.: MODSNOW-Tool: an operational tool for daily snow cover monitoring using MODIS data, Environ. Earth Sci., 75, 1–15, https://doi.org/10.1007/s12665-016-5869-x, 2016.

Gerlitz, L., Steirou, E., Schneider, C., Moron, V., Vorogushyn, S., and Merz, B.: Variability of the cold season climate in Central Asia. Part II: Hydroclimatic predictability, J. Clim., 32, 6015–6033, https://doi.org/10.1175/JCLI-D-18-0892.1, 2019.

Gerlitz, L., Vorogushyn, S., and Gafurov, A.: Climate informed seasonal forecast of water availability in Central Asia: State-

of-the-art and decision making context, Water Secur., 10, 100061, https://doi.org/10.1016/j.wasec.2020.100061, 2020.

Greenwell, B. M., Boehmke, B. C., and McCarthy, A. J.: A Simple and Effective Model-Based Variable Importance Measure, 1–27, 2018.

Huffman, G. J., Stocker, E. F., Bolvin, D. T., Nelkin, E. J., and Tan, J.: GPM IMERG Late Precipitation L3 1 day 0.1 degree x 0.1 degree V06, https://doi.org/https://doi.org/10.5067/GPM/IMERGDL/DAY/06, 2019.

Immerzeel, W. W., Lutz, A. F., Andrade, M., Bahl, A., Biemans, H., Bolch, T., Hyde, S., Brumby, S., Davies, B. J., Elmore, A. C., Emmer, A., Feng, M., Fernández, A., Haritashya, U., Kargel, J. S., Koppes, M., Kraaijenbrink, P. D. A., Kulkarni, A. V., Mayewski, P. A., Nepal, S., Pacheco, P., Painter, T. H., Pellicciotti, F., Rajaram, H., Rupper, S., Sinisalo, A., Shrestha, A. B., Viviroli, D., Wada, Y., Xiao, C., Yao, T., and Baillie, J. E. M.: Importance and vulnerability of the world's water towers, Nature, 577, 364–369, https://doi.org/10.1038/s41586-019-1822-y, 2020.

Kuhn, M.: Building Predictive Models in R Using the caret Package, J. Stat. Softw., 28, 1–26, https://doi.org/10.18637/jss.v028.i05, 2008.

Lehner, F., Wood, A. W., Llewellyn, D., Blatchford, D. B., Goodbody, A. G., and Pappenberger, F.: On the Use of Snow and Climate Information in Statistical Seasonal Streamflow Forecasting, in: 86th Annual Western Snow Conference, 2018.

Mankin, J. S., Viviroli, D., Singh, D., Hoekstra, A. Y., and Diffenbaugh, N. S.: The potential for snow to supply human water demand in the present and future, Environ. Res. Lett., 10, 114016, https://doi.org/10.1088/1748-9326/10/11/114016, 2015.

Mantua, N. J., Hare, S. R., Zhang, Y., Wallace, J. M., and Francis, R. C.: A Pacific Interdecadal Climate Oscillation with Impacts on Salmon Production, Bull. Am. Meteorol. Soc., 78, 1069–1079, https://doi.org/10.1175/1520-0477(1997)078<1069:APICOW>2.0.CO;2, 1997.

Mariotti, A.: How ENSO impacts precipitation in southwest central Asia, Geophys. Res. Lett., 34, 2–6, https://doi.org/10.1029/2007GL030078, 2007.

McNally, A., Jacob, J., Arsenault, K., Slinski, K., Sarmiento, D. P., Hoell, A., Pervez, S., Rowland, J., Budde, M., Kumar, S., Peters-Lidard, C., and Verdin, J. P.: A Central Asia hydrologic monitoring dataset for food and water security applications in Afghanistan, Earth Syst. Sci. Data, 14, 3115–3135, https://doi.org/10.5194/essd-14-3115-2022, 2022.

Mendoza, P. A., Wood, A. W., Clark, E., Rothwell, E., Clark, M. P., Nijssen, B., Brekke, L. D., and Arnold, J. R.: An intercomparison of approaches for improving operational seasonal streamflow forecasts, Hydrol. Earth Syst. Sci., 21, 3915–3935, https://doi.org/10.5194/hess-21-3915-2017, 2017.

Modi, P. A., Small, E. E., Kasprzyk, J., and Livneh, B.: Investigating the Role of Snow Water Equivalent on Streamflow Predictability during Drought, J. Hydrometeorol., 23, 1607–1625, https://doi.org/https://doi.org/10.1175/JHM-D-21-0229.1, 2022.

Muñoz-Sabater, J., Dutra, E., Agust\'\i-Panareda, A., Albergel, C., Arduini, G., Balsamo, G., Boussetta, S., Choulga, M., Harrigan, S., Hersbach, H., Martens, B., Miralles, D. G., Piles, M., Rodr\'\iguez-Fernández, N. J., Zsoter, E., Buontempo, C., and Thépaut, J.-N.: ERA5-Land: a state-of-the-art global reanalysis dataset for land applications, Earth Syst. Sci. Data, 13, 4349–4383, https://doi.org/10.5194/essd-13-4349-2021, 2021.

Murray, S. A.: The Importance of Ensemble Techniques for Operational Space Weather Forecasting, Sp. Weather, 16, 777–783, https://doi.org/https://doi.org/10.1029/2018SW001861, 2018.

Pechlivanidis, I. G., Crochemore, L., Rosberg, J., and Bosshard, T.: What Are the Key Drivers Controlling the Quality of Seasonal Streamflow Forecasts?, Water Resour. Res., 56, e2019WR026987, https://doi.org/https://doi.org/10.1029/2019WR026987, 2020.

Peña-Guerrero, M. D., Umirbekov, A., Tarasova, L., and Müller, D.: Comparing the performance of high-resolution global precipitation products across topographic and climatic gradients of Central Asia, Int. J. Climatol., 0–1, https://doi.org/https://doi.org/10.1002/joc.7548, 2022.

Ropelewski, C. F. and Jones, P. D.: An extension of the Tahiti-Darwin Southern Oscillation Index, Mon. Weather Rev., 115,

1987.

Schär, C., Vasilina, L., Pertziger, F., and Dirren, S.: Seasonal runoff forecasting using precipitation from meteorological data assimilation systems, J. Hydrometeorol., 5, 959–973, https://doi.org/10.1175/1525-7541(2004)005<0959:SRFUPF>2.0.CO;2, 2004.

Syed, F. S., Giorgi, F., Pal, J. S., and Keay, K.: Regional climate model simulation of winter climate over central-southwest Asia, with emphasis on NAO and ENSO effects, Int. J. Climatol., 30, 220–235, https://doi.org/10.1002/joc.1887, 2010.

Troin, M., Arsenault, R., Wood, A. W., Brissette, F., and Martel, J.-L.: Generating Ensemble Streamflow Forecasts: A Review of Methods and Approaches Over the Past 40 Years, Water Resour. Res., 57, e2020WR028392, https://doi.org/https://doi.org/10.1029/2020WR028392, 2021.

Umirbekov, A., Peña-Guerrero, M. D., and Müller, D.: Regionalization of climate teleconnections across Central Asian mountains improves the predictability of seasonal precipitation, Environ. Res. Lett., 17, 55002, https://doi.org/10.1088/1748-9326/ac6229, 2022.

Umirbekov, A., Essery, R., and Müller, D.: GEMS v1.0: Generalizable empirical model of snow accumulation and melt based on daily snow mass changes in response to climate and topographic drivers, Rev., 2023.

Umirbekov, A., Peña-Guerrero, M. D., Didovets, I., Apel, H., Gafurov, A., and Müller, D.: R script and data for the manuscript "The Value of Hydroclimatic Teleconnections for Snowpack-based Seasonal Streamflow Forecasting," https://doi.org/https://doi.org/10.5281/zenodo.11308066, May 2024.

Viviroli, D. and Weingartner, R.: The hydrological significance of mountains: from regional to global scale, Hydrol. Earth Syst. Sci., 8, 1017–1030, https://doi.org/10.5194/hess-8-1017-2004, 2004.

Viviroli, D., Dürr, H. H., Messerli, B., Meybeck, M., and Weingartner, R.: Mountains of the world, water towers for humanity: Typology, mapping, and global significance, Water Resour. Res., 43, https://doi.org/https://doi.org/10.1029/2006WR005653, 2007.

Viviroli, D., Kummu, M., Meybeck, M., Kallio, M., and Wada, Y.: Increasing dependence of lowland populations on mountain water resources, Nat. Sustain., 3, 917–928, https://doi.org/10.1038/s41893-020-0559-9, 2020.

Wang, S., Huang, J., He, Y., and Guan, Y.: Combined effects of the Pacific Decadal Oscillation and El Niño-Southern Oscillation on Global Land Dry-Wet Changes, Sci. Rep., 4, 1–8, https://doi.org/10.1038/srep06651, 2014.

WMO: Guidelines on Seasonal Hydrological Prediction, 2021st ed., World Meteorological Organization, Geneva, 2021.

Xenarios, S., Gafurov, A., Schmidt-Vogt, D., Sehring, J., Manandhar, S., Hergarten, C., Shigaeva, J., and Foggin, M.: Climate change and adaptation of mountain societies in Central Asia: uncertainties, knowledge gaps, and data constraints, Reg. Environ. Chang., 19, 1339–1352, https://doi.org/10.1007/s10113-018-1384-9, 2019.

Zounemat-Kermani, M., Batelaan, O., Fadaee, M., and Hinkelmann, R.: Ensemble machine learning paradigms in hydrology: A review, J. Hydrol., 598, 126266, https://doi.org/https://doi.org/10.1016/j.jhydrol.2021.126266, 2021.